Available online at www.sciencedirect.com

SciVerse ScienceDirect

journal homepage: http://www.elsevier.com/locate/rpor

Original research article

Exit fluence analysis using portal dosimetry in volumetric modulated arc therapy

Prabakar Sukumar[a,*], *Sriram Padmanaban*[a], *Dhanabalan Rajasekaran*[a], *Muniyappan Kannan*[b], *Vivekanandan Nagarajan*[a]

[a] *Medical Physics Department, Cancer Institute (WIA), India*
[b] *Anna University, India*

ARTICLE INFO

Article history:
Received 31 August 2011
Received in revised form 9 May 2012
Accepted 13 June 2012

Keywords:
RapidArc
Exit fluence
Gamma evaluation
EPID
Portal dosimetry

ABSTRACT

Aim: In measuring exit fluences, there are several sources of deviations which include the changes in the entrance fluence, changes in the detector response and patient orientation or geometry. The purpose of this work is to quantify these sources of errors.

Background: The use of the volumetric modulated arc therapy treatment with the help of image guidance in radiotherapy results in high accuracy of delivering complex dose distributions while sparing critical organs. The transit dosimetry has the potential of Verifying dose delivery by the linac, Multileaf collimator positional accuracy and the calculation of dose to a patient or phantom.

Materials and methods: The quantification of errors caused by a machine delivery is done by comparing static and arc picket fence test for 30 days. A RapidArc plan, created for the pelvis site was delivered without and with Rando phantom and exit portal images were acquired. The day to day dose variation were analysed by comparing the daily exit dose images during the course of treatment. The gamma criterion used for analysis is 3% dose difference and 3 mm distance to agreement with a threshold of 10% of maximum dose.

Results: The maximum standard deviation for the static and arc picket fence test fields were 0.19 CU and 1.3 CU, respectively. The delivery of the RapidArc plans without a phantom shows the maximum standard deviation of 1.85 CU and the maximum gamma value of 0.59. The maximum gamma value for the RapidArc plan delivered with the phantom was found to be 1.2. The largest observed fluence deviation during the delivery to patient was 5.7% and the maximum standard deviation was 4.1 CU.

Conclusion: It is found from this study that the variation due to patient anatomy and interfraction organ motion is significant.

* *Corresponding author at*: No. 46 Manimegali Street, East Tambaram, Chennai 600 059, Tamil Nadu, India. Tel.: +91 9789882591.
E-mail address: prabakarsukumar@gmail.com (P. Sukumar).

1507-1367/$ – see front matter © 2012 Greater Poland Cancer Centre. Published by Elsevier Urban & Partner Sp. z o.o. All rights reserved.
http://dx.doi.org/10.1016/j.rpor.2012.06.003

1. Background

The use of the volumetric modulated arc therapy (VMAT) treatment with the help of image guidance in radiotherapy results in high accuracy of delivering complex dose distributions while sparing critical organs. This treatment technique necessitates two or three dimensional (3D) patient specific quality assurance to deliver the dose accurately. Many articles[1–3] described the advantages of the electronic portal imaging device (EPID) as potential for in vivo measurements, point dose measurements and 3D dose verification. The transit (or) projection and non-transit dosimetry are the two categories in the dosimetric verification using the EPID. The non-transit dosimetry is extensively used for the pre-treatment verification without a patient or phantom. The transit dosimetry has the potential of verifying dose delivery by the linac, multileaf collimator positional accuracy and the calculation of dose to a patient or phantom. There has been reports in literature comparing exit fluences with predicted ones[4–9] and also comparing back projected and reconstructed dose with a planned dose distribution within the patient.[10–13] A literature review of the portal imager and dosimetry were described by Van Elmpt et al.[14] The integrated images of portal dosimetry were corrected by General Linear Calibration of the imager (GLAaS) algorithm to convert images to absolute dose measurements in phantom.[15] The 3D dose verification in VMAT was done using gantry angle resolved acquisition or in continuous mode acquisition.[16]

In measuring the exit fluences, there are several sources of deviations, which include changes in the entrance fluence, changes in the detector response and patient orientation or geometry. The magnitude of these deviations during the Intensity Modulated Radiotherapy (IMRT) treatment has been documented.[17] The RapidArc® which is a commercial name for VMAT by Varian, enables IMRT-like dose distributions to be delivered using a single and/or multiple rotation of the gantry.

The sources of the variation were isolated in this work and we investigated the exit fluences by evaluating the magnitude of interfractional dose variation during the RapidArc treatment for pelvic cases.

2. Aim

The purpose of the work is to quantify the exit fluence variation during VMAT delivery due to errors in MLC, gantry position and due to patient geometrical and interfractional organ motion. The acquisition and analysis of exit fluence for each fraction is useful in determining the variation in daily delivered dose and to modify the treatment plan adaptively.

3. Materials and methods

The delivery system used in this study was Varian CLINAC 2100 (Varian Medical Systems, Palo Alto, CA) equipped with a 120-leaf Millenium multi-leaf collimator (MLC) and on-board imager (OBI). A portal imager, amorphous silicon aS1000 EPID (IDU 20 model, Varian Medical Systems, Palo Alto, CA) with an active area of 40 cm × 30 cm consisting of 1024 × 768 pixels which is attached to the machine by Exact arm (E arm) was used to measure the exit fluence. The image acquisition software (IAS3) provides several modes for acquisition. Integrated mode of acquisition is calibrated using a dark field and flood field for 6 MV X-rays. The dark field is corrects leakage charges produced in the imager and the flood field corrects the sensitivity of the imager pixels. The dosimetric calibration was done such that calibration unit (CU) 1 CU = 1 cGy.

This study investigated the daily variations of (1) machine output, (2) MLC positioning, (3) RapidArc fluence, (4) set-up variation and (5) interfractional organ motion. The first three are machine related sources of variations and the other two are the patient induced fluence variability.

3.1. *Machine stability*

Daily portal images were acquired for the field size of 10 cm × 10 cm at the source to detector distance (SDD) of 100 cm for 100 monitor units (MU). The dose rate was 300 MU/min which is being routinely used in clinical situations for conformal and IMRT treatments. In RapidArc, the dose rate varies from 100 MU/min to 600 MU/min. The variation in the dose is found to be less than 2% as in a previous study.[18] The variation obtained was a combination of the accelerator output and the pixel sensitivity. To eliminate the accelerator output variation, images were acquired daily after flood field calibration. Flood field calibration eliminates the daily accelerator output variation. The variations in calibrated units without and with Flood field calibration were analysed over a period of six weeks.

The picket fence test was performed in a static gantry to analyse the fluence variation due to MLC positions at SDD of 150 cm. The picket fence is formed of 1 mm wide regions with high intensity in every 1.5 cm. From the picket fence test, the fluence variation due to MLC positioning was determined. To quantify the variation due to gantry rotation and MLC positioning, arc picket fence test was delivered and portal dose images were acquired at the same SDD. The variation in fluence will be a combination of errors in Gantry and MLC positioning and pixel sensitivity. These tests were performed for a period of six weeks and analysed.

. The standard deviation for the arc Picket fence test was calculated in each pixel and a graph was plotted (Fig. 2

3.2. *Phantom study*

A clinical RapidArc plan for the pelvis site of a patient (P1) was delivered without and with phantom. The test was done for all the five plans which resulted in negligible variation. This may be due to the fact that all the five patients had carcinoma of Uterine Cervix of same stage and all had similar RapidArc plans. Hence, the plan P1 is taken for quantifying the variation in patient positioning and MLC, Gantry positions. The portal dose images were acquired during delivery at SDD of 150 cm. The portal dose images acquired without phantom quantified the variations due to MLC and gantry positions in RapidArc plan.

Computed Tomographic (CT) images were acquired for Anthromorphic (Rando) phantom with 3 mm slice thickness. A verification plan for RapidArc was generated using Rando

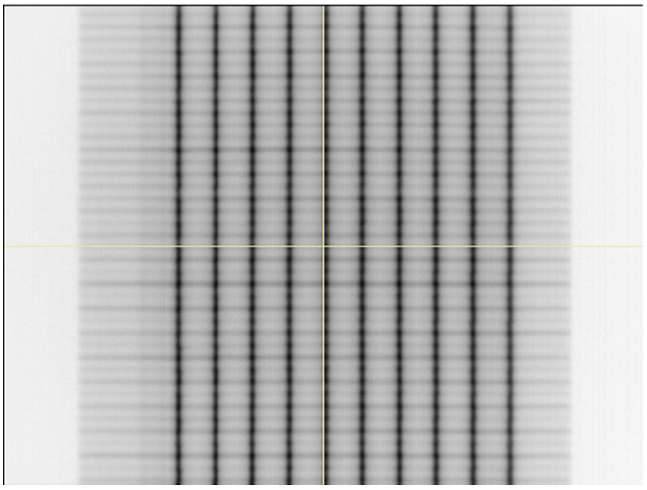

Fig. 1 – EPID image of arc picket fence.

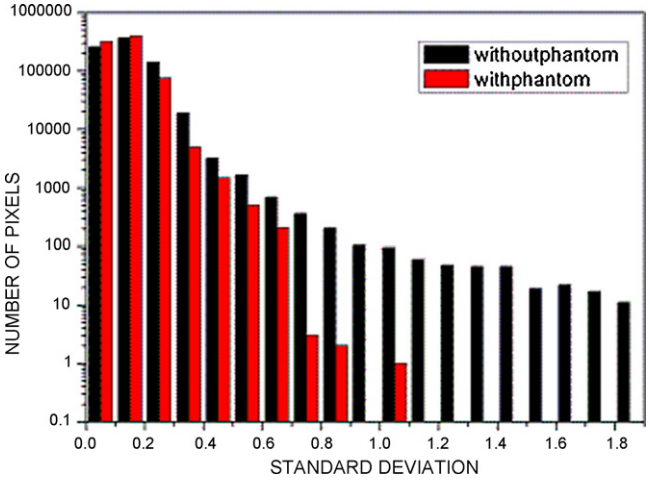

Fig. 3 – Standard deviation without and with phantom.

phantom. Correct phantom position was verified using orthogonal kV images using OBI and delivered exit fluences were recorded. Apart from the gantry and MLC positional errors, the variation in measured exit fluences includes a setup error. The portal dose images without and with phantom were measured over a period of six weeks.

3.3. *Variations due to interfractional organ motion*

To examine the interfractional anatomical variation, exit fluences were measured for the patients during RapidArc treatment. Five patients (P1, P2, P3, P4, and P5) with carcinoma of the uterine cervix with same staging were included for the study. The double arc plans were created with clockwise (CW) and counter clockwise (CCW) arcs from gantry angles ranging from 181.1 to 179.9 (A1) and 179.9 to 181.1 (A2) degrees, respectively, with a collimator angle of 45°. Each plan was also verified by the patient specific quality assurance with the PTW 2D Ionisation chamber array and Octavious phantom, which shows the area failing the gamma value, is less than 5%.

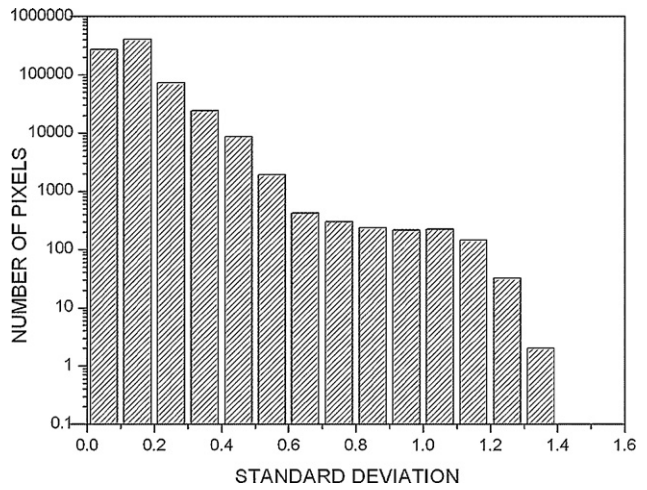

Fig. 2 – Standard deviation arc picket fence.

Before treatment, the patient treatment position was verified by matching the orthogonal kV images with DRR images.

For the phantom and patient study, the standard deviations (SD) were calculated at each pixel for thirty and twenty-five fractions, respectively. Each day variation in exit fluence was plotted with the standard deviation between the corresponding pixels in each fraction in the abscissa and the number of pixels experiencing the standard deviation in the ordinate. First fraction portal image was used as a reference image. The daily portal image were compared with the reference image using the gamma analysis method with criterion 3% dose difference and 3 mm distance to agreement with a threshold value of 10% of maximum value.[19–22] The maximum gamma value and percentage area of gamma failing were analysed for the active area of detector (30 cm × 40 cm). The portal vision software of Eclipse planning system (Varian Medical Systems, Palo Alto, CA) was used for the comparison of the images (version 8.6).

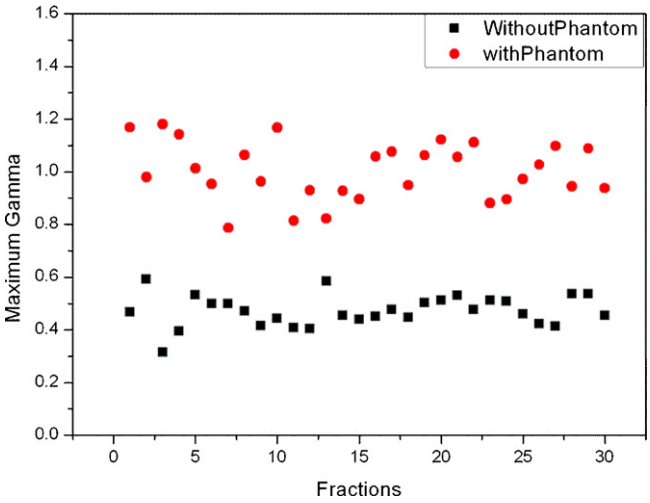

Fig. 4 – Maximum gamma values for period of 30 fractions with and without phantom.

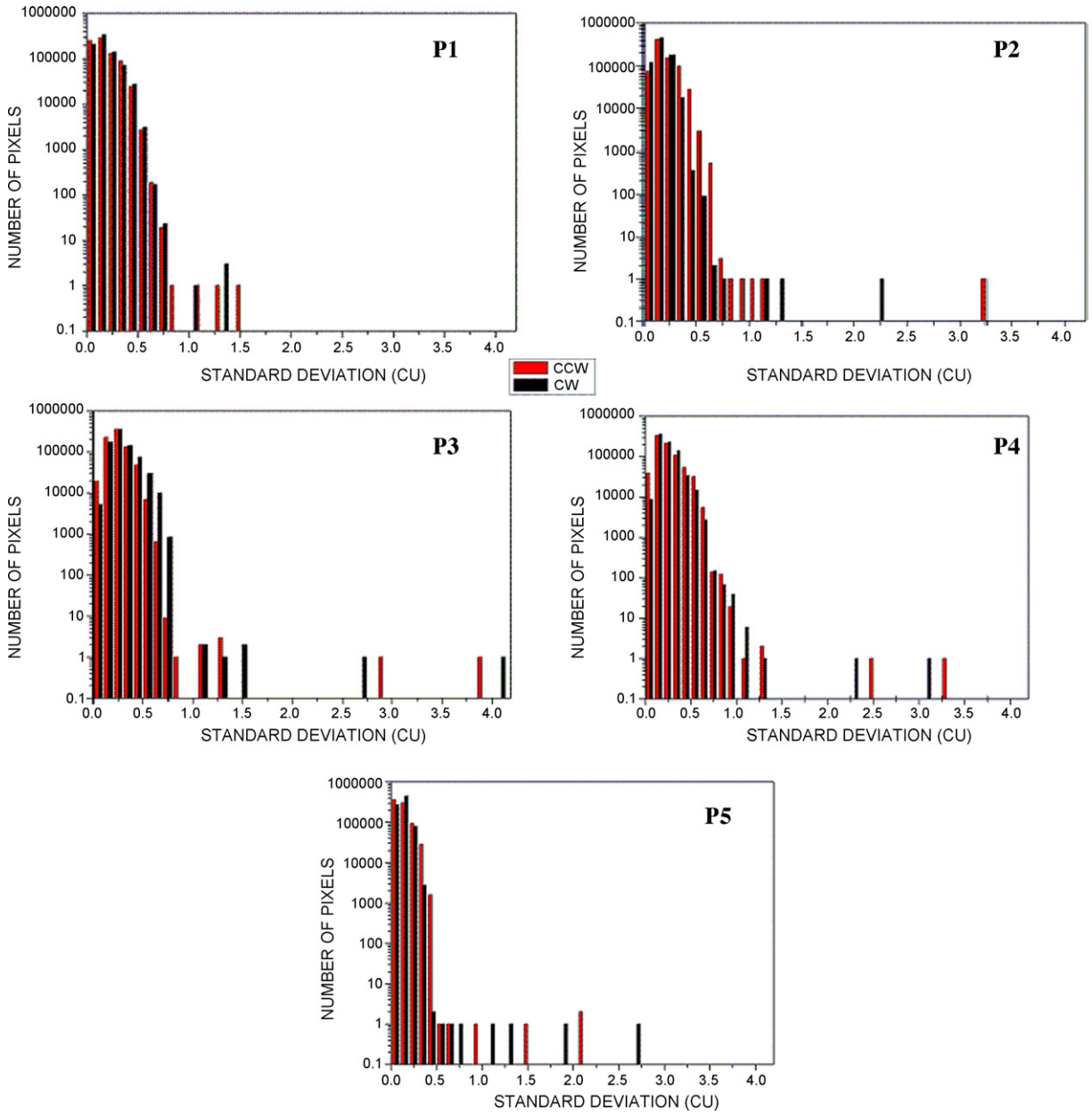

Fig. 5 – Standard deviation between pixels for patients.

4. Results

The calibration unit variation for open field was observed over a period of thirty days without and with flood field calibration. The CU was measured over 10 × 10 pixel area and a maximum variation obtained without and with flood calibration was 1.5% and 0.6%, respectively.

The maximum standard deviation for static Picket fence in each pixel was 0.19 CU and showed a maximum gamma value of 1.61. The maximum area failing gamma criterion was 0.03%. The image of the arc picket fence test is shown in the Fig. 1). The maximum standard deviation observed in a single pixel was 1.3 CU and maximum gamma value was 3.3. The maximum area failing the gamma criteria was 0.1% over a period of six weeks.

When measuring the fluence without phantom or patient, the maximum standard deviation (Fig. 3) was 1.8 CU which occurred in 11 pixels and the maximum gamma value was 0.59 (Fig. 4). The maximum gamma value plotted against fraction number is shown in the Fig. 4. The maximum gamma values were increased for the images acquired with the Rando phantom compared to those acquired without phantom, which is due to scatter from the patient and couch. The maximum standard deviation and maximum gamma value over a period of thirty fractions were 1.1 CU (Fig. 3) and 1.2 (Fig. 4), respectively. The area failing the gamma criterion was less than 0.5% in overall fractions.

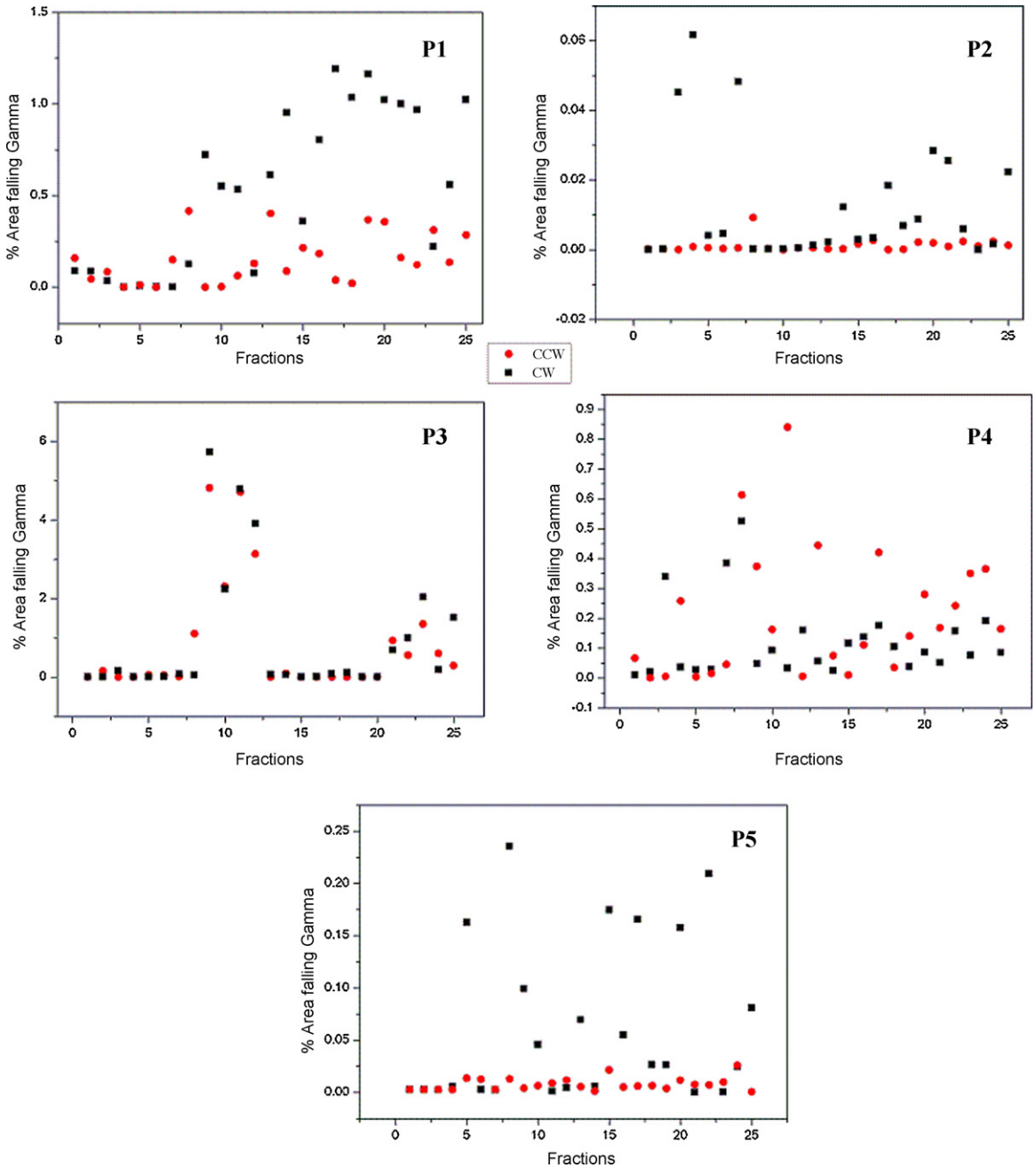

Fig. 6 – Percentage area failing gamma criteria.

For patient study, the area of gamma failing was more significant than the maximum gamma values. Fig. 5 represents the standard deviation for patients between the pixels for twenty-five fractions and Fig. 6 represents the area of Gamma failing for patients. Since the gamma values show large differences in each patient, scale on Y axis vary for the purpose of clarity. The average of the Gamma average was tabulated for picket fence, without phantom, phantom and patient plans (Table 1). The maximum gamma values for patients were plotted against the fraction number (Fig. 7). For the first patient (P1) the maximum gamma values were less than 2 for a period of twenty five days. For the measurements of exit fluence with patients, the maximum area failing the gamma criteria were

Table 1 – Average of γ_{ave} with standard deviation for patients, phantom and without phantom.

Plan	CCW	CW
Picket fence test	0.1330 ± 0.0205	
Without phantom	0.0700 ± 0.0181	0.0646 ± 0.0169
With phantom	0.1151 ± 0.0179	0.0131 ± 0.0153
P1	0.1251 ± 0.0265	0.1373 ± 0.0227
P2	0.1515 ± 0.0461	0.1485 ± 0.0421
P3	0.2636 ± 0.1288	0.2456 ± 0.1202
P4	0.2172 ± 0.0683	0.1988 ± 0.0552
P5	0.1083 ± 0.0112	0.1054 ± 0.0163

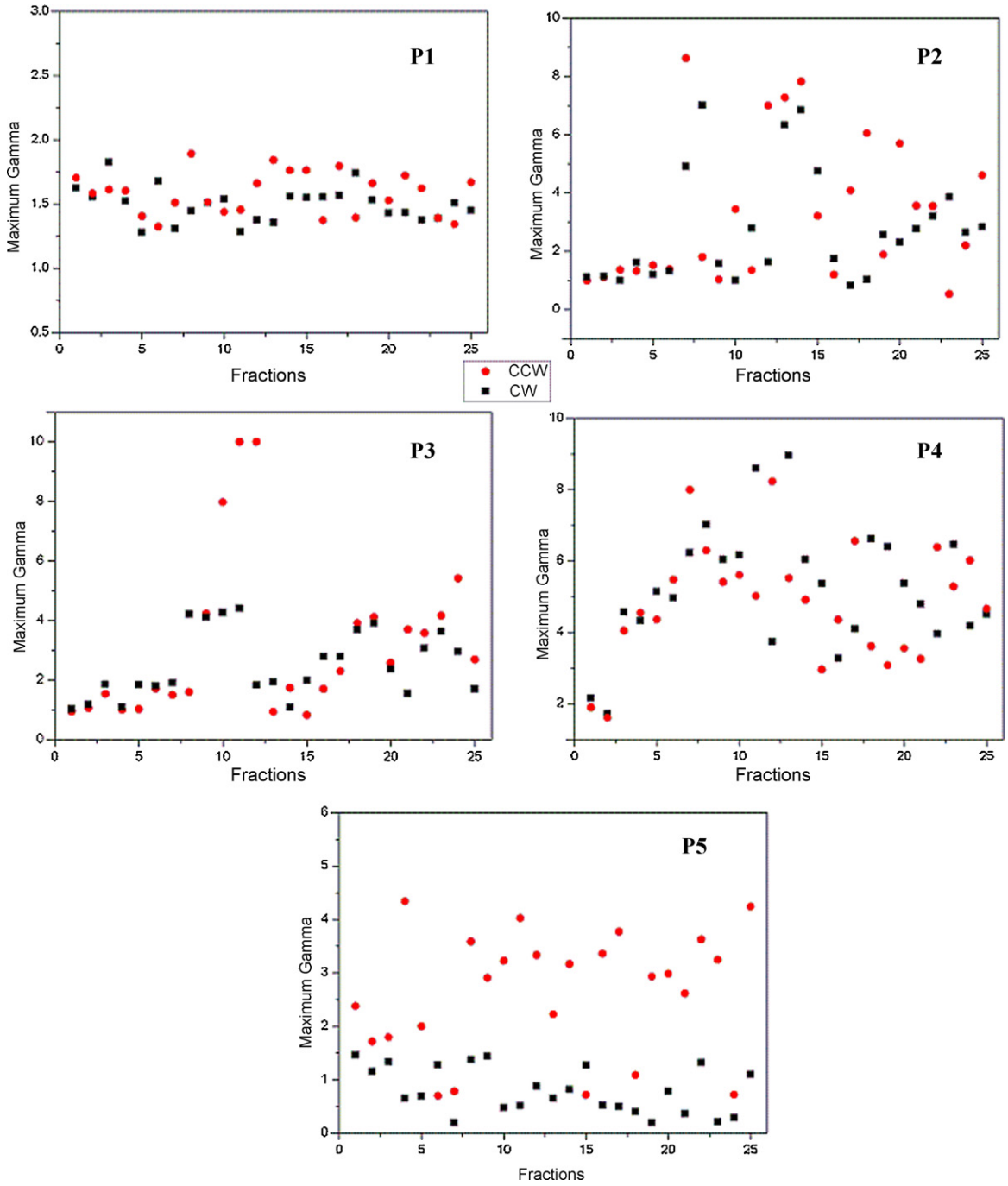

Fig. 7 – Maximum gamma values for patients.

found to be 5.7% and the maximum standard deviation was 4.1 CU (Fig. 8). It is found that, among five patients the area failing gamma criteria was more than 2% for patient 3. The area failing gamma criteria are pronounced due to interfractional anatomical variations.

5. Discussion

Gardner et al. has stated the maximum variation in exit fluence due to a linear accelerator and patient's anatomical changes are about 4% and 9%, respectively in IMRT treatments. In this study, the exit fluence variation due to machine and patients related errors were studied for RapidArc treatments. The sources of variation due to linear accelerator, such as portal imager sensitivity and MLC at different gantry positioning were quantified. The patient related interfractional exit fluence variation due to setup error and anatomical changes were quantified using Rando phantom and patients exit doses images. From the graphs plotted, the deviations due to the machine related sources were less than 0.6 gamma value. The maximum gamma value observed was 1.18 when the

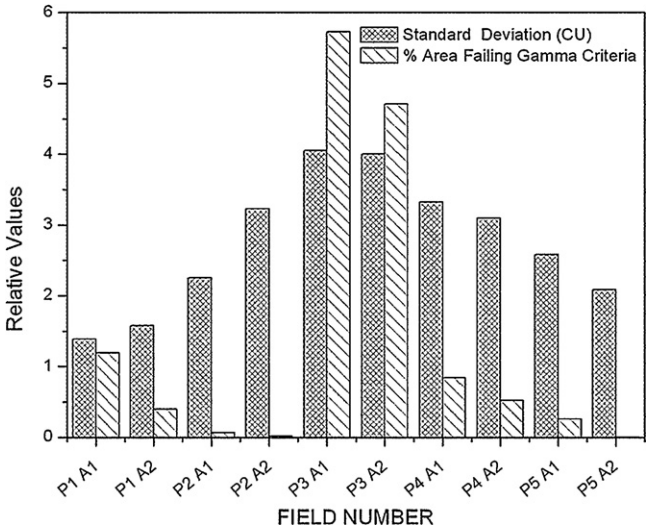

Fig. 8 – Maximum standard deviation and maximum percentage area failing the gamma criteria.

plan was executed to phantom for 30 fractions. In RapidArc patient treatment, the maximum area of gamma failing was 5% (Fig. 6, P3) and maximum gamma was found to be 10. Thus, from analysing the various source of error, the interfractional anatomical variation was found to be predominant. For patient P1 the maximum gamma values found to be less than 2 whereas the area gamma failing criteria is 1.5%. This indicates the minimal movement of organ or proper filling of bladder and rectum produces the lesser variation in the exit fluence. These results agree with the Lee et al. findings.[23]

This study shows the consistency in the patient exit fluence, when treatment positioning was done with the kV images. The sources of deviation are isolated as much as possible. However, there are possibilities that some sources of errors might have gone undetected. This study does not report the deviations in the patient absolute dose and/or variation between planned and measured fluence. The patient's treatment positioning verification was not done with CBCT images, which may further increase the patient setup accuracy. When using exit fluence for dose reconstruction in patient CT images, the variations due to the MLC and output are very small. As the patient related source of error is larger, the dose reconstruction in the cone beam CT images acquired before treatment will be an appropriate method to measure the dose delivered to the patients.

Even with these limitations, portal dose images are used to verify exit dose variation. If the variations of exit dose images exceeds the percentage of area gamma failing is more than 5%, the treatment has to be analysed by taking the CBCT images to verify anatomical positions.

6. Conclusion

The recording and analysis of exit fluence for each fraction is useful in determining the variation in delivered doses. By analysing the results, the errors can be minimised and improve the quality of treatment. The results show that the variation due to interfractional organ motion is greater than the variation caused by machine related sources. With this technique, future clinical developments in adaptive radiation therapy through daily dosimetric measurements of treatment day images are possible. This will be used to verify the accumulated dose delivered to the patient during the entire course of treatment.

Conflict of interest

There is no conflict of interest including any financial, personal or other relationships with other people or organizations within three years of beginning the submitted work that could inappropriately influence, or be perceived to influence, our work.

Financial disclosure

None declared.

REFERENCES

1. Greer PB, Popescu CC. Dosimetric properties of an amorphous silicon electronic portal imaging device for verification of dynamic intensity modulated radiation therapy. *Med Phys* 2003;**30**:1618–27.
2. Van Esch A, Depuydt T, Huyskens DP. The use of an aSi-based EPID for routine absolute dosimetric pre-treatment verification of dynamic IMRT fields. *Radiother Oncol* 2004;**71**:223–34.
3. van Elmpt W, Nijsten S, Mijnheer B, Dekker A, Lambin P. The next step in patient-specific QA: 3D dose verification of conformal and intensity-modulated RT based on EPID dosimetry and Monte Carlo dose calculations. *Radiother Oncol* 2008;**86**:86–92.
4. Kroonwijk M, Pasma KL, Quint S, Koper PC, Visser AG, Heijmen BJ. In vivo dosimetry for prostate cancer patients using an electronic portal imaging device (EPID): demonstration of internal organ motion. *Radiother Oncol* 1998;**49**:125–32.
5. Pasma KL, Heijmen BJ, Kroonwijk M, Visser AG. Portal dose image (PDI) prediction for dosimetric treatment verification in radiotherapy: I. An algorithm for open beams. *Med Phys* 1998;**25**:830–40.
6. McCurdy BM, Pistorius S. A two-step algorithm for predicting portal dose images in arbitrary detectors. *Med Phys* 2000;**27**:2109–16.
7. McCurdy BM, Luchka K, Pistorius S. Dosimetric investigation and portal dose image prediction using an amorphous silicon electronic portal imaging device. *Med Phys* 2001;**28**:911–24.
8. van Elmpt W, Nijsten S, Mijnheer B, Minken A. Experimental verification of a portal dose prediction model. *Med Phys* 2005;**32**:2805–18.
9. Vieira SC, Dirkx ML, Heijmen BJ, de Boer HC. SIFT: a method to verify the IMRT fluence delivered during patient treatment using an electronic portal imaging device. *Int J Radiat Oncol Biol Phys* 2004;**60**:981–93.
10. Partridge M, Ebert M, Hesse BM. IMRT verification by three-dimensional dose reconstruction from portal beam measurements. *Med Phys* 2002;**29**:1847–58.
11. Louwe RJ, Damen EM, van Herk M, Minken AW, Törzsök O, Mijnheer BJ. Three-dimensional dose reconstruction of breast

cancer treatment using portal imaging. *Med Phys* 2003;**30**:2376–89.
12. Jarry G, Verhaegen F. Patient-specific dosimetry of conventional and intensity modulated radiation therapy using a novel full Monte Carlo phase space reconstruction method from electronic portal images. *Phys Med Biol* 2007;**52**:2277–99.
13. McDermott LN, Wendling M, Nijkamp J, et al. 3D in vivo dose verification of entire hypo-fractionated IMRT treatments using an EPID and cone-beam CT. *Radiother Oncol* 2008;**86**:35–42.
14. van Elmpt W, McDermott L, Nijsten S, Wendling M, Lambin P, Mijnheer B. A literature review of electronic portal imaging for radiotherapy dosimetry. *Radiother Oncol* 2008;**88**:289–309.
15. Nicolini G, Vanetti E, Clivio A, et al. The GLAaS algorithm for portal dosimetry and quality assurance of RapidArc, intensity modulated rotational therapy. *Radiat Oncol* 2008;**3**:24.
16. Bakhtiari M, Kumaraswamy L, Bailey DW, de Boer S, Malhotra HK, Podgorsak MB. Using an EPID for patient-specific VMAT quality assurance. *Med Phys* 2011;**38**:1366.
17. Gardner JK, Clews L, Gordon JJ, Wang S, Greer PB, Siebers JV. Comparison of sources of exit fluence variation for IMRT. *Phys Med Biol* 2009;**54**:N451–8.
18. Prabakar S, Sriram P, Prakash J, Syam Kumar SA, Vivekanandan N. A study on dosimetric properties of electronic portal imaging device and its use as quality assurance tool in Volumetric Modulated Arc Therapy. *Rep Pract Oncol Radiother* 2011;**16**:248–55.
19. Low DA, Harms WB, Mutic S, Purdy JA. A technique for quantitative evaluation of dose distribution. *Med Phys* 1998;**25**:656–61.
20. Andenna C, Benassi M, Caccia B, Marzi S, Pedrini M, Zicari C. Comparison of dose distributions in IMRT planning using the gamma function. *J Exp Clin Cancer Res* 2006;**25**(2): 229–34.
21. McDermott LN, Wendling M, van Asselen B, et al. Clinical experience with EPID dosimetry for prostate IMRT pre-treatment dose verification. *Med Phys* 2006;**33**(10):3921–30.
22. Lee C, Menk F, Cadman P, Greer PB. A simple approach to using an amorphous silicon EPID to verify IMRT planar dose maps. *Med Phys* 2009;**36**:984.
23. Lee L, Le QT, Xing L. Retrospective IMRT dose reconstruction based on cone-beam CT and MLC log-file. *Int J Radiat Oncol Biol Phys* 2008;**70**:634–44.